

**NJC****Tetranuclear Iron Carbonyl Complexes with a Central Tin Atom: Relationship to Iron Carbonyl Carbides**

Journal:	<i>New Journal of Chemistry</i>
Manuscript ID	NJ-ART-03-2018-001434.R1
Article Type:	Paper
Date Submitted by the Author:	22-May-2018
Complete List of Authors:	Gong, Xiaoli; Hangzhou Dianzi University Zhu, Liyao; Hangzhou Dianzi University, College of Electronic Information Zhao, Jufeng; Hangzhou Dianzi University Cui, Guangmang; Hangzhou Dianzi University Lu, Xinmiao; Hangzhou Dianzi University Xie, Yaoming; University of Georgia, Center for Computational Chemistry King, R.; University of Georgia, Chemistry

SCHOLARONE™
Manuscripts

5/18

Tetranuclear Iron Carbonyl Complexes with a Central Tin Atom: Relationship to Iron Carbonyl Carbides

Xiaoli Gong,^a Liyao Zhu,^{*a} Jufeng Zhao,^a Guangmang Cui,^a Xinmiao Lu,^a
Yaoming Xie,^b and R. Bruce King,^{*b}

^a*College of Electronics and Information, Hangzhou Dianzi University,
Hangzhou, Zhejiang 310018, P. R China*

^b*Department of Chemistry and Center for Computational Quantum Chemistry, University
of Georgia, Athens, Georgia 30602, USA*

e-mails: rbking@chem.uga.edu and zly@hdu.edu.cn

Abstract

The two tetranuclear iron carbonyl systems $EFe_4(CO)_n$ ($E = Sn, C$) containing central group 14 interstitial atoms differ in that spiro-pentane-like $SnFe_4(CO)_{16}$ has been synthesized in the tin system whereas the butterfly $CFe_4(CO)_{13}$, with three fewer carbonyl groups is the carbonyl-richest tetranuclear iron carbonyl carbide that has been synthesized. In order to clarify this point, the complete $SnFe_4(CO)_n$ ($n = 16, 15, 14, 13, 12$) series has been studied by density functional theory for comparison with earlier similar studies on their $CFe_4(CO)_n$ analogues. The experimentally observed spiro-pentane-like $Sn[Fe_2(CO)_8]_2$ structure is found to be the lowest energy structure for the $SnFe_4(CO)_{16}$ system as it is for the experimentally unknown $CFe_4(CO)_{16}$ system. Loss of a CO group from $Sn[Fe_2(CO)_8]_2$ joins the two $Fe_2(CO)_8$ units by a third Fe–Fe bond to give an $SnFe_4(CO)_{15}$ structure with a bonded four-atom Fe–Fe–Fe–Fe chain. Further CO loss from $SnFe_4(CO)_{15}$ adds a fourth Fe–Fe bond in the lowest energy $SnFe_4(CO)_{14}$ structure. The lowest energy $SnFe_4(CO)_{13}$ structure is analogous to that of the experimentally known iron carbonyl carbide $CFe_4(CO)_{13}$ with a central Fe_4 butterfly having five Fe–Fe bonds. The energetics of CO dissociation from the $EFe_4(CO)_n$ ($E = C, Sn; n = 16, 15, 14, 13$) species account for the experimentally observed differences between the systems with central tin and central carbon atoms. Thus for the tin systems the CO dissociation energy from $SnFe_4(CO)_{16}$ is relatively high at ~ 50 kcal/mol consistent with its experimental observation as a stable species. However, for the tetranuclear iron carbonyl carbides $CFe_4(CO)_n$ the CO dissociation energies of the species with more than 13 CO groups are all very small or even negative suggesting $CFe_4(CO)_{13}$ to be the carbonyl-richest viable iron tetracarbonyl carbide consistent with experiment.

1. Introduction

Very stable metal carbonyl complexes containing direct metal-tin bonds have long been known. The first such compounds were obtained from metal carbonyl anions and organotin halides.¹ Although most of the early chemistry was done with the tetracarbonylcobalt anion, Hieber and Breu in 1957 also reported the reaction of $\text{K}_2\text{Fe}(\text{CO})_4$ with $n\text{Bu}_2\text{SnCl}_2$ to give a species $n\text{Bu}_2\text{SnFe}(\text{CO})_4$, later shown to be a dimer with a central four-membered Fe_2Sn_2 ring (Figure 1).² Related $[\text{R}_2\text{SnFe}(\text{CO})_4]_2$ dimers were obtained from thermal reactions of $\text{Fe}(\text{CO})_5$ with various organotin compounds.^{3,4} Under more forcing conditions reactions of organotin compounds with $\text{Fe}(\text{CO})_5$ resulted in removal of all alkyl and/or aryl groups from the tin atom leading to a species of stoichiometry $\text{Sn}[\text{Fe}_2(\text{CO})_8]_2$. This species was shown to have a spiro-pentane structure (Figure 1) with four iron-tin bonds to two $\text{Fe}_2(\text{CO})_8$ units, each containing an iron-iron bond.⁵ This structure can formally be regarded as a tetrahedral $\text{Sn}(\text{IV})$ derivative of the known $\text{Fe}_2(\text{CO})_8^{2-}$ dianion in which the iron atom has the favored 18-electron configuration. Thus stripping all $\text{Sn}-\text{C}$ bonds from the central tin atom in reactions of organotin compounds with iron carbonyls leads to the pairwise coupling of the external $\text{Fe}(\text{CO})_4$ units by forming iron-iron bonds. Similar spiro-pentane-like $\text{E}[\text{Fe}_2(\text{CO})_8]_2$ ($\text{E} = \text{Si}, \text{Pb}$) species have also been synthesized with silicon,⁶ germanium, and lead⁷ as the central atoms.

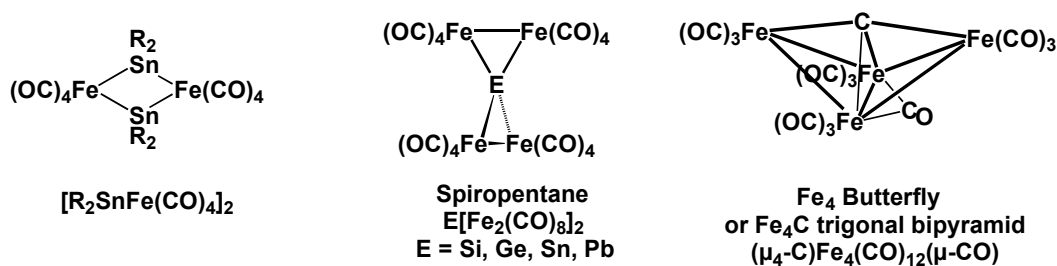


Figure 1. The first organotin complexes of iron carbonyl $(\text{R}_2\text{SnFe}(\text{CO})_4)_2$; comparison of the experimentally spiro-pentane-like $\text{E}\{\text{Fe}_2(\text{CO})_8\}_2$ structures with the carbonyl-poorer stable tetranuclear iron carbonyl carbide structure $(\mu_4\text{-C})\text{Fe}_4(\text{CO})_{12}(\mu\text{-CO})$.

This tetranuclear iron carbonyl tin chemistry stands in direct contrast with tetranuclear iron carbonyl carbide chemistry. Thus the stable tetranuclear iron carbonyl carbide has the stoichiometry $\text{CFe}_4(\text{CO})_{13}$ and structurally consists of a tin atom imbedded into an Fe_4 butterfly with five $\text{Fe}-\text{Fe}$ bonds.⁸ An analogous tin compound of

stoichiometry $\text{SnFe}_4(\text{CO})_{13}$ or $\text{SnFe}_4(\text{CO})_n$ ($n = 15, 14$) with intermediate numbers of carbonyl groups remains unknown. Furthermore, a density functional theory study⁹ shows spiropentane-like $\text{C}[\text{Fe}_2(\text{CO})_8]_2$ structures analogous to the experimental $\text{Sn}[\text{Fe}_2(\text{CO})_8]_2$ structure to be the lowest energy structures for the stoichiometry $\text{CFe}_4(\text{CO})_{16}$. However, the calculated CO dissociation energies for the $\text{CFe}_4(\text{CO})_n$ ($n = 16, 15, 14$) carbonyl richer structures than the known $\text{CFe}_4(\text{CO})_{13}$ suggest such structures to be disfavored relative to CO dissociation.

In order to understand the experimentally observed differences between the $\text{CFe}_4(\text{CO})_n$ and $\text{SnFe}_4(\text{CO})_n$ systems, we have now performed a theoretical study of the $\text{SnFe}_4(\text{CO})_n$ ($n = 16, 15, 14, 13, 12$) systems. This paper reports our results thereby enabling a comparison between the tetranuclear iron carbonyl derivatives with central carbon and those with central tin atoms. In particular the different patterns of the CO dissociation energies for the two sequences $\text{EFe}_4(\text{CO})_n$ ($\text{E} = \text{C}, \text{Sn}$) are able to account for $\text{CFe}_4(\text{CO})_{13}$ and $\text{Sn}[\text{Fe}_2(\text{CO})_8]_2$ being the stable species, respectively.

2. Theoretical Methods

Two density functional theory (DFT) methods were used in this paper. The BP86 method combines Becke's 1988 exchange functional (B) with Perdew's 1986 gradient-corrected correlation functional (P86)^{10, 11} and usually provides better vibrational frequencies.^{12,13} Thus, we discuss the vibrational frequencies predicted by the BP86/ DZP method in the work. The second functional is M06-L, a meta-GGA DFT method, developed by Truhlar and Zhao.¹⁴ They suggest M06-L for transition-metal compounds, since it predicts relative energies closer to experimental values. Thus, we adopt the energy orderings predicted by the M06-L method, but list the results from the BP86 method in the Supporting Information. Standard double- ζ plus polarization (DZP) and triple- ζ plus polarization (TZP) basis sets were adopted in the present study. The TZP and DZP basis sets are designated as (10s6p2d1f/5s3p2d1f) and (9s5p1d/4s2p1d) for carbon and oxygen, (16s13p6d2f1g/9s6p3d2f1g) and (15s12p5d1f/8s6p2d1f) for iron, and (20s16p9d2f1g/9s7p4d2f1g) and (19s15p8d1f/8s6p3d1f) for tin, respectively.

The geometries of all structures were fully optimized using the two DFT methods, i.e., M06-L/TZP and BP86/DZP. Harmonic vibrational frequencies and the corresponding infrared intensities were determined by evaluating analytically the second derivatives of the energy with respect to the nuclear coordinates. All computations were performed with the Gaussian 09 program package.¹⁵ The ultra fine grid (99, 590) was the default for evaluating two-electron integrals numerically.¹⁶ The tight (10^{-8} hartree) designation was the default for the self-consistent-field (SCF) convergence except for **16S-1** and **16S-2**.

Natural bond orbital (NBO) analyses^{17,18,19} were carried out using the two DFT methods to provide information on the chemical bonding in these system. All of the predicted triplet structures in the present study are found to have negligible spin contamination, with $S(S+1)$ values close to the ideal 2.0.

A given $\text{SnFe}_4(\text{CO})_n$ structure is designated as **nA-c** where **n** is the number of CO groups, **c** orders the structures according to their relative energies, and **A** indicates whether the structure is a singlet (**S**) or triplet (**T**). Thus the lowest energy singlet structure of $\text{SnFe}_4(\text{CO})_{16}$ is designated **16S-1**.

3. Results and Discussion

3.1. $\text{SnFe}_4(\text{CO})_n$ ($n = 16$ to 12) structures. The SnFe_4 skeletons in the $\text{SnFe}_4(\text{CO})_n$ ($n = 16$ to 12) compounds studied in the present paper are of five different types, namely spiropentane, distorted spiropentane, twisted spiropentane, distorted triangular pyramidal, and butterfly (Figure 2). Each skeletal type has four Fe-Sn bonds except the twisted spiropentane type, which has only three Fe-Sn bonds. In the spiropentane and twisted spiropentane skeleton the four iron atoms are partitioned into two bonded Fe_2 pairs. The twisted spiropentane skeleton can be dissected into a Sn(II) ligand with an SnFe_2 three-membered ring using a lone pair on the tin atom to form a dative bond with an Fe_2 unit involving the other two iron atoms. The distorted spiropentane skeleton has these two bonded Fe_2 pairs linked by an additional Fe-Fe bond to form a bonded Fe_4 chain. The distorted triangular pyramidal skeleton and butterfly skeleton have four and five Fe-Fe bonds, respectively. All of the $\text{SnFe}_4(\text{CO})_n$ ($n = 12$ to 16) structures are predicted to be genuine minima with all real vibrational frequencies except for **16S-2**, which is predicted to have two small imaginary frequencies of $41i$ and $15i \text{ cm}^{-1}$.

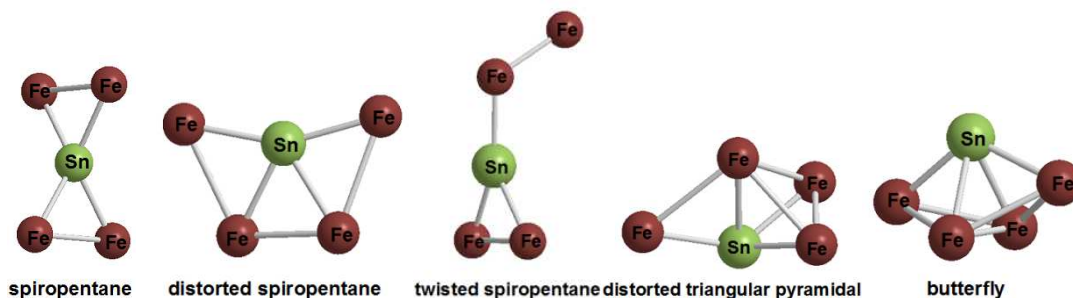


Figure 2. The fundamental SnFe_4 skeletons in the $\text{SnFe}_4(\text{CO})_n$ ($n = 16$ to 12) compounds.

3.1.1 $\text{SnFe}_4(\text{CO})_{16}$ structures. Two low-energy singlet $\text{SnFe}_4(\text{CO})_{16}$ structures, namely the unbridged D_{2d} structure **16S-1** and the doubly CO-bridged C_{2v} structure **16S-2**, were found. (Figure 3). Structure **16S-1** corresponds to the experimental structure as determined by X-ray crystallography.⁵ The symmetry equivalent two Fe–Fe and four Sn–Fe distances in **16S-1** of 2.872 and 2.520 Å, respectively, are very close to the experimental Fe–Fe and Sn–Fe bond distances of 2.87 and 2.54 Å in $\text{SnFe}_4(\text{CO})_{16}$. These Fe–Fe and Sn–Fe bond distances in **16S-1** coupled with their WBIs of 0.19 and 0.37 suggest formal single bonds, thereby giving each iron atom the favored 18-electron configuration.

The doubly CO-bridged C_{2v} spiro-pentane $\text{SnFe}_4(\text{CO})_{16}$ structure **16S-2**, lying 7.3 kcal/mol in energy above **16S-1**, has two Fe–Fe bonds and four Sn–Fe bonds. In **16S-2** the unbridged Fe1–Fe2 distance of 2.876 Å is essentially identical to that in **16S-1**. The doubly bridged Fe3–Fe4 distance at 2.601 Å is significantly shorter than the unbridged Fe1–Fe2 distance by 0.275 Å, which is the typical effect of two bridging CO groups across a metal-metal bond. In **16S-2** the WBI of 0.18 for the Fe1–Fe2 bond and that of 0.14 for the Fe3–Fe4 both suggest formal single bonds, thereby giving each iron atom the favored 18-electron configuration. The bridging $\nu(\text{CO})$ frequencies in **16S-2** of 1859 and 1876 cm^{-1} are significantly lower than the lowest terminal $\nu(\text{CO})$ frequency by $\sim 200 \text{ cm}^{-1}$ in accord with expectation.

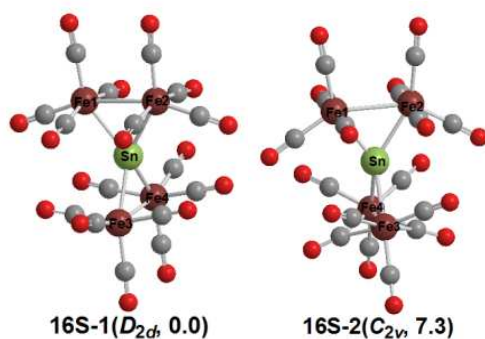


Figure 3. Optimized $\text{SnFe}_4(\text{CO})_{16}$ structures. Relative energies (in kcal/mol) by M06-L are shown under each structure.

3.1.2. $\text{SnFe}_4(\text{CO})_{15}$ structures. Two singlet structures **15S-1** and **15S-2** and one triplet structure **15T-1** for $\text{SnFe}_4(\text{CO})_{15}$ were found within 18 kcal/mol of the global minimum (Figure 4). The lowest energy structure **15S-1** is predicted to have a distorted spiro-pentane SnFe_4 skeleton (Figure 4). Thus, in contrast to the $\text{SnFe}_4(\text{CO})_{16}$ structures **16S-1** and **16S-2**, the SnFe_4 skeleton in **15S-1** is distorted to bring Fe2 and Fe3 close enough to form a third iron-iron bond of length 2.747 Å which is bridged by one of the

CO groups. Thus there are three iron-iron bonds, four iron-tin bonds and one bridging CO group in **15S-1**. The four iron atoms and one tin atom in **15S-1** are nearly planar with equivalent Fe1-Fe2 and Fe3-Fe4 distances of 2.917 Å. For the iron-tin bonds the Sn-Fe2/Sn-Fe3 and Sn-Fe1/Sn-Fe4 distances are 2.543 Å and 2.442 Å, respectively. The Fe1-Fe2/Fe3-Fe4, Fe2-Fe3, Sn-Fe2/Sn-Fe3 and Sn-Fe1/Sn-Fe4 bond distances in **15S-1** coupled with their WBIs of 0.14, 0.19, 0.31 and 0.44, respectively, suggest formal single bonds in all cases, thereby giving each iron atom the favored 18-electron configuration. The $\nu(\text{CO})$ frequency of 1834 cm^{-1} for the bridging CO group in **15S-1** lies 244 cm^{-1} below the lowest terminal $\nu(\text{CO})$ frequency,

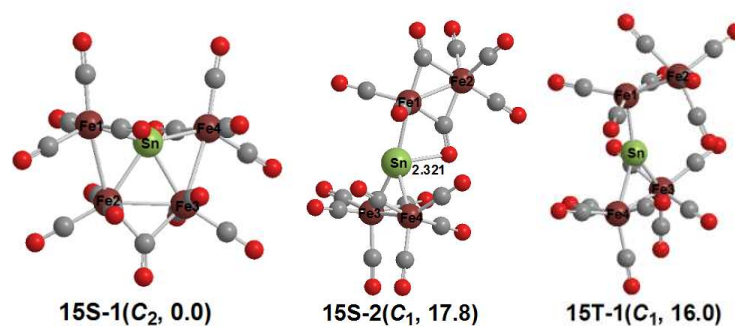


Figure 4. The optimized $\text{SnFe}_4(\text{CO})_{15}$ structures.

The $\text{SnFe}_4(\text{CO})_{15}$ structure **15S-2**, lying 17.8 kcal/mol above **15S-1**, is a C_1 singlet twisted spirocyclic structure with two iron-iron bonds, three iron-tin bonds, and two bridging CO groups (Figure 4). Structure **15S-2** is a very unusual structure that can be dissected into a $\text{Sn}(\text{II})$ ligand of the type $:\text{SnFe}_2(\text{CO})_8$ with a lone pair on the tin atom coordinating to an iron atom in an $\text{Fe}_2(\text{CO})_7$ unit. The $\text{Sn}\rightarrow\text{Fe}$ dative bond in **15S-2** is of length 2.431 Å with a WBI value of 0.39. One of the bridging CO groups in the $\text{Fe}_2(\text{CO})_7$ unit “bites back” to the $\text{Sn}(\text{II})$ atom by forming a dative $\text{O}\rightarrow\text{Sn}$ bond as noted above with a bonding distance of 2.321 Å. This CO group has an unusually low $\nu(\text{CO})$ frequency of 1540 cm^{-1} whereas the other bridging CO group in **15S-2** has a more typical bridging $\nu(\text{CO})$ frequency of 1849 cm^{-1} . Thus the $:\text{SnFe}_2(\text{CO})_8$ unit with exclusively terminal CO groups can be considered to be amphoteric by functioning as a Lewis base towards an $\text{Fe}_2(\text{CO})_7$ unit but as a Lewis acid towards one of the bridging CO oxygen atoms of the $\text{Fe}_2(\text{CO})_7$ unit. The $\text{Fe1}=\text{Fe2}$ distance of 2.431 Å in the $\text{Fe}_2(\text{CO})_7$ unit combined with its WBI of 0.37 suggests the formal double bond required to give each iron atom in this $\text{Fe}_2(\text{CO})_7$ unit the favored 18-electron configuration after considering the electron pair from the $:\text{SnFe}_2(\text{CO})_8$ “ligand.” The $\text{Fe3}-\text{Fe4}$ distance of 2.847 Å within the $:\text{SnFe}_2(\text{CO})_8$ ligand is $\sim 0.4\text{ Å}$ longer than the $\text{Fe1}=\text{Fe2}$ distance in the $\text{Fe}_2(\text{CO})_7$ unit

and corresponds to a WBI of 0.19 which is approximately half that of the Fe1=Fe2 WBI. This indicates the formal Fe3–Fe4 single bond in the :SnFe₂(CO)₈ ligand required to give both iron atoms the favored 18-electron configuration.

The triplet SnFe₄(CO)₁₅ structure **15T-1**, lying 16.0 kcal/mol above **15S-1**, is a C₁ triplet structure with two iron-iron bonds, three iron-tin bonds and all terminal CO groups (Figure 4). Structure **15T-1** has a twisted spiro pentane skeleton, similar to the SnFe₄ skeleton of **15S-2**. However, **15T-1** lacks a dative bond from one of the bridging CO groups to the tin atom as indicated by exclusively non-bonding Sn···O distances. The Sn→Fe dative bond in **15T-1** of length 2.410 Å with a WBI of 0.57 is very similar to that in **15S-2** discussed above except with a higher WBI owing to the tin coordination number of three because of the lack of a Sn···O bond. The Fe1–Fe2 distance of 2.490 Å in **15T-1** is similar to the Fe1–Fe2 distance of 2.431 Å in **15S-2**. However, the WBI of 0.21 for the Fe1–Fe2 interaction in **15T-1** is much less than the WBI of 0.37 in **15S-2**. Interpreting the Fe1–Fe2 bond in **15T-1** as a formal single bond gives these iron atoms a 17-electron configuration thereby providing the two unpaired electrons for the triplet spin state.

3.1.3. SnFe₄(CO)₁₄. Three singlet structures and two low-energy triplet structures were found for SnFe₄(CO)₁₄ within 20 kcal/mol of the lowest energy structure **14S-1** (Figure 5). Structure **14S-1** is a singlet structure with four iron-iron bonds, four iron-tin bonds, and one bridging CO group connecting the Fe3 and Fe4 atoms. The tin atom in **14S-1** is bonded to four iron atoms, leading to a distorted triangular pyramidal skeleton (Figure 5). In **14S-1** the Fe1–Fe2, Fe3–Fe4, Fe2–Fe3, and Fe2–Fe4 distances of 2.973 Å, 2.691 Å, 2.805 Å, and 2.806 Å, respectively, with Wiberg bond indices (WBIs) ranging from 0.15 to 0.23, can be considered as formal single bonds forming an Fe₃ triangle with an externally bonded fourth iron atom. The Sn-Fe1/Sn-Fe4 distances in **14S-1** of 2.455 Å/2.443 Å are shorter than the Sn-Fe2/Sn-Fe3 distances in **14S-1** of 2.576 Å/2.495 Å consistent with their WBIs of 0.53/0.48 and 0.30/0.38, respectively. However, they can all be considered as single bonds to give each iron atom the favored 18-electron configuration. The single bridging CO group in **14S-1** exhibits a ν(CO) frequency at 1849 cm⁻¹, which lies 230 cm⁻¹ below the lowest terminal ν(CO) frequency in accord with expectation.

The singlet SnFe₄(CO)₁₄ structure **14S-2**, lying 8.9 kcal/mol in energy above **14S-1**, has two pairs of bonded Fe₂ units, four iron-tin bonds and two bridging CO groups connecting the Fe3 and Fe4 atoms (Figure 5). The spiro pentane SnFe₄ skeleton of **14S-2** is similar to the SnFe₄ skeleton of **16S-1**. The central tin atom in **14S-2** is bonded to an Fe₂(CO)₈ unit and an Fe₂(CO)₆ unit with the two bridging CO groups in the latter unit.

The Fe1–Fe2 distance of 2.817 Å in the Fe₂(CO)₈ unit of **14S-2** with a corresponding WBI of 0.19 is very similar to the Fe–Fe distances in the SnFe₄(CO)₁₆ structure **16S-1**. This Fe1–Fe2 interaction can thus be considered as a formal single bond thereby giving each iron atom the favored 18-electron configuration. The Fe3=Fe4 distance of 2.352 Å in the Fe₂(CO)₆ unit of **14S-2** is at least 0.058 Å shorter than the formal iron-iron double bonds in **15S-2** and **15T-1**. However, its WBI of only 0.32 in **14S-2** is smaller than the WBIs of 0.37 and 0.57 for the Fe=Fe double bonds in **15S-2** and **15T-1**, respectively. Considering the Fe3≡Fe4 interaction in the Fe₂(CO)₆ unit of **14S-2** as a formal triple bond gives these iron atoms the favored 18-electron configuration. However, the Fe3–Fe4 interaction in the Fe₂(CO)₆ unit of **14S-2** as only a single bond can give each iron atom only a 16-electron configuration. The actual situation in **14S-2** could be a resonance hybrid between these two possibilities. The two bridging ν(CO) frequencies in **14S-2** of 1899 and 1903 cm⁻¹ are ~170 cm⁻¹ below the lowest terminal ν(CO) frequency in accord with expectation.

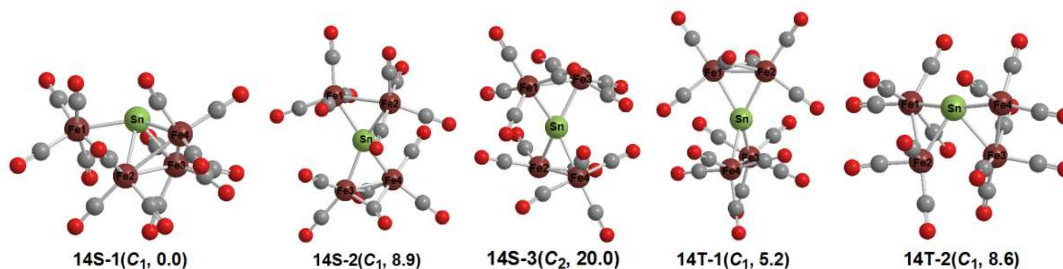


Figure 5. Optimized SnFe₄(CO)₁₄ structures.

The SnFe₄(CO)₁₄ structure **14S-3**, lying 20.0 kcal/mol in energy above **14S-1**, is an Sn[Fe₂(CO)₇]₂ structure with an SnFe₄ spiro-pentane skeleton and exclusively terminal CO groups (Figure 5). The iron-iron distances of 2.736 Å in **14S-3** with WBIs of 0.20 can be interpreted as formal single bonds. This provides Fe1 and Fe4 bearing four CO groups with the favored 18-electron configuration. However, Fe2 and Fe3, each bearing only three CO groups have only 16-electron configurations. The Fe(CO)₃ units with iron atoms Fe2 and Fe3 each have a gap in the coordination sphere corresponding to their 16-electron configurations. The Sn[Fe₂(CO)₇]₂ structure **14S-3** can be derived from the Sn[Fe₂(CO)₈]₂ structure **16S-1** by removal of a terminal CO group from each Fe₂(CO)₈ unit.

The C₁ triplet SnFe₄(CO)₁₄ structure **14T-1**, lying 5.2 kcal/mol in energy above **14S-1**, is a spiro-pentane Sn[Fe₂(CO)₈][Fe₂(CO)₆] structure with two semibridging carbonyl groups connecting the Fe1 and Fe2 atoms in the Fe₂(CO)₈ unit with short Fe-C

distances of ~ 1.8 Å and long Fe-C distances of ~ 2.2 Å. The Fe1=Fe2 distance of 2.427 Å in the $\text{Fe}_2(\text{CO})_6$ unit of **14T-1** is similar to the formal iron-iron double bonds in **15S-2** and **15T-1** although its WBI is rather low at 0.22. The Fe3–Fe4 bond length of 2.850 Å with a WBI of 0.18 in the $\text{Fe}_2(\text{CO})_8$ unit of **14T-1** is similar to both Fe–Fe bonds in the $\text{Sn}[\text{Fe}_2(\text{CO})_8]_2$ structure **16S-1** and thus can be interpreted as a formal single bond. Considering the Fe1=Fe2 bond in **14T-1** as a formal double bond and the Fe3–Fe4 bond as a formal single bond gives Fe3 and Fe4 the favored 18-electron configuration but Fe1 and Fe2 only 17 electron configurations. The latter two iron atoms in **14T-1** thus provide the two unpaired electrons for the triplet spin state. The two semibridging CO groups in **14T-1** exhibits $\nu(\text{CO})$ frequencies at 1885 and 1897 cm^{-1} , which are approximately 180 cm^{-1} below the lowest terminal $\nu(\text{CO})$ frequency in accord with expectation.

The triplet SnFe_4 structure **14T-2**, lying 8.6 kcal/mol in energy above **14S-1**, is a distorted spiro pentane $\text{Sn}[\text{Fe}_2(\text{CO})_7]_2$ structure with all terminal carbonyl groups (Figure 5). The distortion brings the $\text{Fe}(\text{CO})_3$ portions of the $\text{Fe}_2(\text{CO})_7$ units closer together with an Fe2 and Fe3 bonding distance of 3.004 Å. Interpreting the three Fe–Fe interactions in **14S-1** as formal single bonds gives the iron atoms of the two $\text{Fe}(\text{CO})_4$ units the favored 18-electron configuration. However, each iron atom in the two $\text{Fe}(\text{CO})_3$ units has a 17-electron configuration thereby providing the two unpaired electrons for the triplet spin state of **14T-2**.

3.1.4. $\text{SnFe}_4(\text{CO})_{13}$. The singlet $\text{SnFe}_4(\text{CO})_{13}$ structure **13S-1** is a very favorable structure since it lies 19.6 kcal/mol in energy below the next lowest energy structure, namely the triplet structure **13T-1**. Structure **13S-1** has a butterfly skeleton (Figure 2) with five iron-iron bonds, four tin-iron bonds, and one bridging carbonyl group (Figure 6). Each iron atom bears three terminal CO groups. The thirteenth CO group in **13S-1** bridges the unique Fe–Fe bond corresponding to the body of the butterfly. This bridging CO group exhibits a $\nu(\text{CO})$ frequency at 1874 cm^{-1} , which lies 190 cm^{-1} below the lowest terminal $\nu(\text{CO})$ frequency in accord with expectation. The four unbridged Fe–Fe bonds from the butterfly body to a wingtip have lengths of ~ 2.7 Å with WBIs of 0.22. The single CO-bridged Fe–Fe bond within the butterfly body is ~ 0.1 Å shorter at ~ 2.6 Å but has a slightly lower WBI of 0.18, probably related to some delocalization involving the bridging CO group. Considering all the iron-iron and tin-iron bonds in **13S-1** as formal single bonds gives the four iron atoms the favorable 18-electron configuration provided that the two wingtip iron atoms with two Fe–Fe bonds bear formal negative charges and the two body iron atoms with three Fe–Fe bonds bear formal positive charges. Replacing

the tin atom in the $\text{SnFe}_4(\text{CO})_{13}$ structure **13S-1** with a carbide carbon atom gives the experimentally known⁸ iron carbonyl carbide structure $\text{CFe}_4(\text{CO})_{13}$.

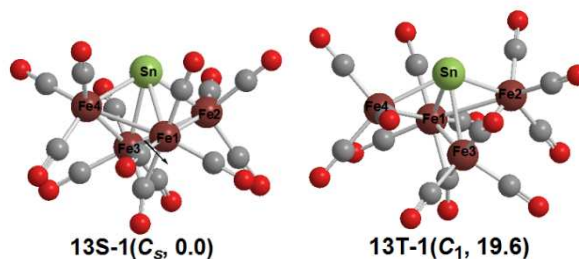


Figure 6. The optimized $\text{SnFe}_4(\text{CO})_{13}$ structures.

The Fe–Sn–Fe angle of 120.9° in the $\text{SnFe}_4(\text{CO})_{13}$ structure **13S-1** deviates considerably from linearity in contrast to the nearly linear Fe–C–Fe angle of 176.1° (B3LYP/DZP) or 174.7° (BP86/DZP) in its carbide analogue $\text{CFe}_4(\text{CO})_{13}$. Therefore **13S-1** is best interpreted as a trigonal bipyramidal SnFe_4 cluster with an equatorial tin atom. Because of the significantly bent Fe–Sn–Fe angle the tin atom has a formal external lone pair and thus is a donor of two skeletal electrons. This makes **13S-1** a 12 skeletal electron system after adding the two skeletal electrons provided by each $\text{Fe}(\text{CO})_3$ unit and two more skeletal electrons from the “extra” carbonyl group to the two skeletal electrons provided by the tin vertex. Thus **13S-1** is a $2n + 2$ (for $n = 5$) skeletal electron system consistent with its deltahedral structure by the Wade-Mingos rules^{20,21,22} and with a similar skeletal electron count to the experimentally known²³ trigonal bipyramidal carborane $\text{C}_2\text{B}_3\text{H}_5$.

The triplet $\text{SnFe}_4(\text{CO})_{13}$ **13T-1**, lying 19.6 kcal/mol in energy above **13S-1**, can be derived from the butterfly structure **13S-1** by stretching one of the four Fe–Fe bonds beyond bonding distance (Figure 6). The two iron atoms at the ends of the stretched Fe–Fe bond thus attain a 17-electron configuration thereby providing the two unpaired electrons for the triplet spin state of **13T-1**. The bridging CO group in **13T-1** exhibits a $\nu(\text{CO})$ frequency of 1858 cm^{-1} , which lies $\sim 200\text{ cm}^{-1}$ below the lowest terminal $\nu(\text{CO})$ frequency in accord with expectation.

3.1.5. $\text{SnFe}_4(\text{CO})_{12}$. Two singlet low-energy structures **12S-1** and **12S-2** and one low-energy triplet structure **12T-1** for $\text{SnFe}_4(\text{CO})_{12}$ lie within 10 kcal/mol of the lowest energy structure (Figure 7). The lowest energy $\text{SnFe}_4(\text{CO})_{12}$ structure **12T-1** is a singly CO-bridged triplet spin state structure with an SnFe_4 butterfly skeleton having five Fe–Fe bonds and four Sn–Fe bonds. The semibridging CO groups in **12T-1** have short Fe–C distances of $\sim 1.8\text{ \AA}$ and long Fe–C distances of ranging from ~ 2.1 to $\sim 2.4\text{ \AA}$. These

semibridging CO groups exhibit $\nu(\text{CO})$ frequencies at 1841, 1867, and 1924 cm^{-1} which are all well below the lowest terminal $\nu(\text{CO})$ frequency in accord with expectation. The Fe1-Fe3 and Fe2-Fe3 edges bridged by CO groups of lengths 2.395 and 2.435 Å in **12T-1** are significantly shorter than the unbridged Fe1-Fe3, Fe2-Fe4, and Fe1-Fe4 edges of lengths 2.622, 2.686, and 2.703 Å, respectively. The two short Fe-Fe edges have WBIs of 0.27 and 0.30 whereas the three longer Fe-Fe edges have smaller WBIs ranging from 0.16 to 0.18. Considering all of these five Fe-Fe interactions in **12T-1** as formal single bonds gives two of the four iron atoms the favored 18-electron configuration. However, the other two iron atoms in **12T-1** have only 17-electron configurations accounting for the triplet spin state of **12T-1**.

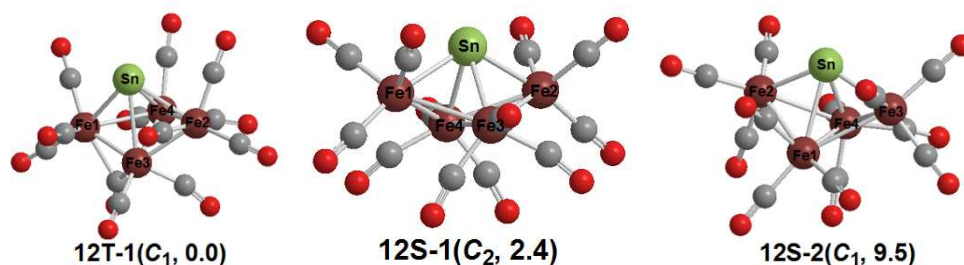


Figure 7. The optimized $\text{SnFe}_4(\text{CO})_{12}$ structures.

The C_2 singlet $\text{SnFe}_4(\text{CO})_{12}$ structure **12S-1**, lying only 2.4 kcal/mol in energy above **12T-1**, also has a butterfly skeleton with five iron-iron bonds and four tin-iron bonds and all terminal CO groups (Figure 7). All five Fe-Fe bonds in **12S-1** have lengths between 2.63 and 2.75 Å and WBIs between 0.15 to 0.23. None of these Fe-Fe distances and corresponding WBIs suggest formal double bonds. However, for all of the iron atoms in **12S-1** to have the favored 18-electron configuration there must be one double bond somewhere in the central SnFe_4 butterfly. Structure **12S-1** could be a resonance hybrid between canonical structures having a formal Fe=Fe bond for one of the butterfly edges and formal Fe-Fe single bonds for the four other butterfly edges.

The next singlet $\text{SnFe}_4(\text{CO})_{12}$ structure **12S-2**, lying 9.5 kcal/mol above **12T-1**, has a similar SnFe_4 butterfly skeleton to **12S-1** but with two semibridging CO groups rather than all terminal CO groups (Figure 7). The semibridging CO groups in **12S-2** have short Fe-C distances of ~ 1.8 Å and long Fe-C distances of 2.3 Å (Figure 7).

3.2. Thermochemistry. The thermochemical predictions in Table 1 and 2 provide insights into the viability of the $\text{SnFe}_4(\text{CO})_n$ ($n = 16$ to 13) derivatives. Table 1 reports the dissociation energies for removing one CO group from the lowest energy $\text{SnFe}_4(\text{CO})_n$ (n

= 16 to 13) structures according to the following equations:

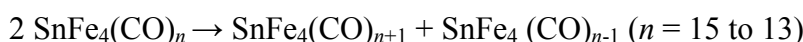


The CO dissociation energies of $\text{SnFe}_4(\text{CO})_n$ ($n = 16$ to 13) are all predicted to be at least 19.5 kcal/mol. However, the CO dissociation energy of $\text{SnFe}_4(\text{CO})_{16}$ of 49.8 kcal/mol is much higher than those of $\text{SnFe}_4(\text{CO})_n$ ($n = 15, 14$) suggesting that $\text{SnFe}_4(\text{CO})_{16}$ is very stable with respect to carbonyl dissociation. This agrees with experiment, since only $\text{SnFe}_4(\text{CO})_{16}$ has been synthesized to date. The carbonyl dissociation energy of $\text{SnFe}_4(\text{CO})_{13}$ is also high at 46.6 kcal/mol so that $\text{SnFe}_4(\text{CO})_{13}$ analogous to the known⁸ $\text{CFe}_4(\text{CO})_{13}$ could be another synthesis target. These CO dissociation energies can be compared with the experimental CO dissociation energies of 27, 41, and 37 kcal/mol for $\text{Ni}(\text{CO})_4$, $\text{Fe}(\text{CO})_5$, and $\text{Cr}(\text{CO})_6$, respectively.²⁴

Table 1. Bond dissociation energies (kcal/mol) after zero-point energy corrections (kcal/mol) for successive removal of carbonyl groups from the lowest energy optimized $\text{SnFe}_4(\text{CO})_n$ ($n = 16$ to 13) structures by the M06-L method.

	M06-L
$\text{SnFe}_4(\text{CO})_{16}$ (16S-1) \rightarrow $\text{SnFe}_4(\text{CO})_{15}$ (15S-1) + CO	49.8
$\text{SnFe}_4(\text{CO})_{15}$ (15S-1) \rightarrow $\text{SnFe}_4(\text{CO})_{14}$ (14S-1) + CO	23.6
$\text{SnFe}_4(\text{CO})_{14}$ (14S-1) \rightarrow $\text{SnFe}_4(\text{CO})_{13}$ (13S-1) + CO	19.8
$\text{SnFe}_4(\text{CO})_{13}$ (13S-1) \rightarrow $\text{SnFe}_4(\text{CO})_{12}$ (12T-1) + CO	46.6

Table 2 reports the energies for the following disproportionation reactions:



The disproportionation of $\text{SnFe}_4(\text{CO})_{15}$ into $\text{SnFe}_4(\text{CO})_{16} + \text{SnFe}_4(\text{CO})_{14}$ is an exothermic process by 26.2 kcal/mol. Similarly, the disproportionation of $\text{SnFe}_4(\text{CO})_{14}$ into $\text{SnFe}_4(\text{CO})_{15} + \text{SnFe}_4(\text{CO})_{13}$ is an exothermic process, albeit with a much lower energy release of only 3.8 kcal/mol. This suggests that neither $\text{SnFe}_4(\text{CO})_{15}$ nor $\text{SnFe}_4(\text{CO})_{14}$ are viable species. In contrast, the disproportionation of $\text{SnFe}_4(\text{CO})_{13}$ into $\text{SnFe}_4(\text{CO})_{14}$ and $\text{SnFe}_4(\text{CO})_{12}$ is an endothermic process by 26.8 kcal mol⁻¹, suggesting that $\text{SnFe}_4(\text{CO})_{13}$ might be a stable molecule.

Table 2. Disproportionation energies after zero-point energy corrections (kcal/mol) for the reactions $2\text{SnFe}_4(\text{CO})_n \rightarrow \text{SnFe}_4(\text{CO})_{n+1} + \text{SnFe}_4(\text{CO})_{n-1}$ ($n = 15$ to 13) with the lowest energy structures by the M06-L method.

	M06-L
$2 \text{SnFe}_4(\text{CO})_{15}$ (15S-1) \rightarrow $\text{SnFe}_4(\text{CO})_{16}$ (16S-1) + $\text{SnFe}_4(\text{CO})_{14}$ (14S-1)	-26.2
$2 \text{SnFe}_4(\text{CO})_{14}$ (14S-1) \rightarrow $\text{SnFe}_4(\text{CO})_{15}$ (15S-1) + $\text{SnFe}_4(\text{CO})_{13}$ (13S-1)	-3.8
$2 \text{SnFe}_4(\text{CO})_{13}$ (13S-1) \rightarrow $\text{SnFe}_4(\text{CO})_{14}$ (14S-1) + $\text{SnFe}_4(\text{CO})_{12}$ (12T-1)	26.8

4. Conclusions

The lowest energy structures of the tetranuclear tin-iron carbonyls $\text{SnFe}_4(\text{CO})_n$ ($n = 16, 15, 14, 13, 12$) follow a similar pattern to those of the corresponding iron carbonyl carbides $\text{CFe}_4(\text{CO})_n$. Thus for both systems the lowest energy $\text{EFe}_4(\text{CO})_{16}$ structures are of the type $\text{E}[\text{Fe}_2(\text{CO})_8]_2$ with a central EFe_4 spiro-pentane network and an iron-iron bond in each $\text{Fe}_2(\text{CO})_8$ unit. The tin derivative $\text{Sn}[\text{Fe}_2(\text{CO})_8]_2$ is thus formally a Sn(IV) derivative of the known $\text{Fe}_2(\text{CO})_8^{2-}$ anion. The lowest energy structures for the $\text{SnFe}_4(\text{CO})_n$ ($n = 15, 14, 13$) species have $18-n$ Fe-Fe bonds thereby providing each iron atom with the preferred 18-electron configuration. Thus for the $\text{SnFe}_4(\text{CO})_{15}$ system the central SnFe_4 spiro-pentane unit is distorted to form a third Fe-Fe bond connecting the two $\text{Fe}_2(\text{CO})_8$ units thereby leading to a bonded Fe-Fe-Fe-Fe chain. Further CO loss from $\text{SnFe}_4(\text{CO})_{15}$ adds a fourth Fe-Fe bond in the lowest energy $\text{SnFe}_4(\text{CO})_{14}$ structure. The lowest energy $\text{SnFe}_4(\text{CO})_{13}$ structure is analogous to that of the experimentally known iron carbonyl carbide $\text{CFe}_4(\text{CO})_{13}$ with a central Fe_4 butterfly having five Fe-Fe bonds. Further closure of the Fe_4 unit in the low-energy $\text{SnFe}_4(\text{CO})_{12}$ structures does not occur by forming a sixth Fe-Fe bond thereby giving a central Fe_4 tetrahedron. Instead the central Fe_4 butterfly is maintained in low-energy singlet and triplet $\text{SnFe}_4(\text{CO})_{12}$ structures.

The energetics of CO dissociation from the $\text{EFe}_4(\text{CO})_n$ ($\text{E} = \text{C, Sn}; n = 16, 15, 14, 13$) account for the experimentally observed differences between the systems with central tin and central carbon atoms. Thus for the tin systems the CO dissociation energy from $\text{SnFe}_4(\text{CO})_{16}$ is relatively high at 49.8 kcal/mol consistent with its experimental observation as a stable species. The CO dissociation products $\text{SnFe}_4(\text{CO})_n$ ($n = 15, 14$) are not viable with respect to $\text{SnFe}_4(\text{CO})_{16} + \text{SnFe}_4(\text{CO})_{13}$. However, $\text{SnFe}_4(\text{CO})_{13}$ has a significant CO dissociation energy of 46.6 kcal/mol. This suggests the possibility of synthesizing $\text{SnFe}_4(\text{CO})_{13}$ analogous to the known $\text{CFe}_4(\text{CO})_{13}$. For the tetranuclear iron carbonyl carbides $\text{CFe}_4(\text{CO})_n$ the CO dissociation energies of the species with more than 13 CO groups are all very small or even negative suggesting $\text{CFe}_4(\text{CO})_{13}$ to be the carbonyl-richest viable iron tetracarbonyl carbide consistent with experiment.

This theoretical study also resulted in the identification of a higher energy $\text{SnFe}_4(\text{CO})_{15}$ structure **15S-2** which can be dissected into a derivative of $\text{Fe}_2(\text{CO})_8$ with a central Fe=Fe double bond in which one of the CO group has been replaced by a $:\text{SnFe}_2(\text{CO})_8$ "ligand" containing a bivalent Sn(II) ligand with a lone pair on the tin atom. Although **15S-2** is a relatively high energy $\text{SnFe}_4(\text{CO})_{15}$ structure, lying ~ 18 kcal/mol above its isomer **15S-1**, its observation suggests the possibility of other

transition metal systems where the lowest energy structure has such a bivalent tin $:\text{SnFe}_2(\text{CO})_8$ ligand.

Acknowledgement

This work is supported by Zhejiang Science and Technology program project (2017C31061, 2013C31073) and Key laboratory of RF Circuits and Systems (Hangzhou Dianzi University), Ministry of Education. The work is also partly supported by Zhejiang Provincial Natural Science Foundation of China (LY18F050007), the key technologies R&D Program of Guangzhou City (201704020182), the National Natural Science Foundation of China (61405052, 61405053). We are also indebted to the U. S. National Science Foundation (Grants CHE-1057466, CHE-1054286, and CHE-1361178) for support of this work.

Supporting Information. Tables S1 to S15: Theoretical Cartesian coordinates for the structures of $\text{SnFe}_4(\text{CO})_n$ ($n = 16$ to 12) using the M06-L/TZP and BP86/DZP methods; Tables S16 to S30: Theoretical harmonic vibrational frequencies for the structures of $\text{SnFe}_4(\text{CO})_n$ ($n=16$ to 12) using the M06-L/TZP and BP86/DZP methods; Tables S31 to S34: Metal-metal distances, natural population analysis natural charges, metal electron configuration, formal metal-metal bond orders, and WBIs for the $\text{SnFe}_4(\text{CO})_n$ ($n = 16$ to 12) structures using the M06-L/TZP and BP86/DZP methods; Table S35. $\nu(\text{CO})$ frequencies and infrared intensities (in km/mol) for the $\text{SnFe}_4(\text{CO})_n$ ($n = 16$ to 12) structures calculated by using the BP86/DZP method; Complete Gaussian09 reference (reference 15).

Literature References

- (1) Hieber, W.; Breu, R. Über Organometallcobaltcarbonyle. *Chem. Ber.* **1957**, *90*, 1270–1274.
- (2) Hein, F.; Jehn, W. Über Organoeisen- und Kobaltcarbonyle. *Chem. Ber.* **1965**, *684*, 4–9.
- (3) King, R. B.; Stone, F. G. A. The reaction between iron pentacarbonyl and tetraorganotin compounds. *J. Am. Chem. Soc.*, **1960**, *82*, 3833–3835.
- (4) Cotton, J. D.; Duckworth, J.; Knox, S. A.; Lindley, R. F.; Paul, I.; Stone, F. G. A.; Woodward, P. Tin-iron carbonyl clusters and sequences. *Chem. Commun.* **1966**, 253–254.
- (5) Lindley, P. F.; Woodward, P. Crystal and molecular structure of tetrakis-[tetracarbonyliron]tin. *J. Chem. Soc. A (London)* **1967**, 382–392.
- (6) Anema, S. G.; Barris, G. C.; MacKay, K. M.; Nicholson, B. K. Improved syntheses of $M[Fe_2(CO)_8]_2$ (M = silicon, germanium, or tin) and the x-ray crystal structure of $Si[Fe_2(CO)_8]_2$. *J. Organometal. Chem.* **1988**, *350*, 207–215.
- (7) Whitmire, K. H.; Lagrone, C. B.; Churchill, M. R.; Fettinger, J. C.; Robinson, B. H. Oxidation/reduction chemistry of iron carbonyl clusters containing germanium, tin, or lead: crystal and molecular structures of $[Et_4N]_2[Fe_3(CO)_9(\mu_3-CO)-(\mu_3-Ge\{Fe(CO)_4\})]$ and $Pb[Fe_2(CO)_8]_2$. *Inorg. Chem.* **1987**, *26*, 3491–3499.
- (8) Bradley, J. S.; Ansell, G. B.; Leonowicz, M. E.; Hill, E. W. Synthesis and molecular structure of μ_4 -carbido- μ_2 -carbonyl-dodecacarbonyltetrairon, a neutral iron butterfly cluster bearing an exposed carbon atom. *J. Am. Chem. Soc.* **1981**, *103*, 4968–4970.
- (9) Gong, X.; Zhu, L.; Yang, J.; Gao, X.; Li, Q.-s.; Xie, Y.; King, R. B.; Schaefer, H. F. From spiroentane to butterfly and tetrahedral structures in tetranuclear iron carbonyl carbide chemistry. *New J. Chem.*, **2014**, *38*, 3762–3769.
- (10) Becke, A. D. Density-functional exchange-energy approximation with correct asymptotic behavior. *Phys. Rev. A*, **1988**, *38*, 3098–3100.
- (11) Perdew, J. P. Density-functional approximation for the correlation energy of the inhomogeneous electron gas. *Phys. Rev. B*, **1986**, *33*, 8822–8824.
- (12) Feng, X.; Gu, J.; Xie, Y.; King, R. B.; Schaefer, H. F.. Homoleptic carbonyls of the second-row transition metals: Evaluation of Hartree–Fock and density functional theory methods. *J. Chem. Theor. Comput.* **2007**, *3*, 1580–1587.
- (13) Zhao, S.; Li, Z. H.; Wang, W. N.; Li, Z.; Liu, Z. P.; Fan, K. N.; Xie, Y. M.; Schaefer, H. F. Is the uniform electron gas limit important for small Ag clusters? Assessment of different density functionals for Ag_n ($n \leq 4$). *J. Chem. Phys.*, **2006**, *124*, 184102.
- (14) Zhao, Y.; Truhlar, D. G. The M06 suite of density functionals for main group thermochemistry, thermochemical kinetics, noncovalent interactions, excited states, and transition elements: two new functionals and systematic testing of four M06-class functionals and 12 other functionals. *Theor. Chem. Accts.* **2008**, *120*, 215–241.

- (15) Gaussian 09, Revision A.01, M. J. Frisch, G. W. Trucks, H. B. Schlegel, G. E. Scuseria, M. A. Robb, J. R. Cheeseman, G. Scalmani, V. Barone, B. Mennucci, G. A. Petersson, H. Nakatsuji, M. Caricato, X. Li, H. P. Hratchian, A. F. Izmaylov, J. Bloino, G. Zheng, J. L. Sonnenberg, M. Hada, M. Ehara, K. Toyota, R. Fukuda, J. Hasegawa, M. Ishida, T. Nakajima, Y. Honda, O. Kitao, H. Nakai, T. Vreven, J. A. Montgomery, Jr., J. E. Peralta, F. Ogliaro, M. Bearpark, J. J. Heyd, E. Brothers, K. N. Kudin, V. N. Staroverov, R. Kobayashi, J. Normand, K. Raghavachari, A. Rendell, J. C. Burant, S. S. Iyengar, J. Tomasi, M. Cossi, N. Rega, J. M. Millam, M. Klene, J. E. Knox, J. B. Cross, V. Bakken, C. Adamo, J. Jaramillo, R. Gomperts, R. E. Stratmann, O. Yazyev, A. J. Austin, R. Cammi, C. Pomelli, J. W. Ochterski, R. L. Martin, K. Morokuma, V. G. Zakrzewski, G. A. Voth, P. Salvador, J. J. Dannenberg, S. Dapprich, A. D. Daniels, O. Farkas, J. B. Foresman, J. V. Ortiz, J. Cioslowski, and D. J. Fox, Gaussian, Inc., Wallingford CT, 2009.
- (16) Papas, B. N.; Schaefer, H. F. Concerning the precision of standard density functional programs: Gaussian, Molpro, NWChem, Q-Chem, and Gamess. *J. Mol. Struct.* **2006**, *768*, 175-181.
- (17) NBO 5.0: Glendening, E. D.; Badenhoop, J. K.; Reed, A. E.; Carpenter, J. E.; Bohmann, J. A.; Morales, C. M.; Weinhold, F., Theoretical Chemistry Institute, University of Wisconsin, Madison, WI, 2001.
- (18) Reed, A. E.; Curtiss, L. A.; Weinhold, F. Intermolecular interactions from a natural bond orbital donor-acceptor viewpoint. *Chem. Rev.* **1988**, *88*, 899–926.
- (19) Wiberg, K. B. Application of Pople-Santry-Segal CNDO method to cyclopropylcarbinyl and cyclobutyl cation and to bicyclobutane. *Tetrahedron* **1968**, *24*, 1083–1096.
- (20) Wade, K. The structural significance of the number of skeletal bonding electron-pairs in carboranes, the higher boranes and borane anions, and various transition-metal carbonyl cluster compounds. *J. Chem. Soc. D: Chem. Commun.*, **1971**, 792–793.
- (21) Mingos, D. M. P. A general theory for cluster and ring compounds of the main group and transition elements. *Nature Phys. Sci.*, **1972**, *236*, 99–102.
- (22) Mingos, D. M. P. Polyhedral skeletal electron pair approach. *Accts. Chem. Res.*, **1984**, *17*, 311–319.
- (23) McNeill, E. A.; Gallaher, K. L.; Scholer, F. R.; Bauer, S. H. Molecular structure of 1,5-dicarba-closo-pentaborane-(5) and 1,6-dicarba-closo-hexaborane(6) by gas-phase electron diffraction. *Inorg. Chem.* **1973**, *12*, 108–111.
- (24) Sunderlin, L.; Wang, D.; Squires, R. R. Bond strengths in first-row transition metal carbonyl anions. *J. Am. Chem. Soc.* **1993**, *115*, 12060-12070.

Table of Contents Entry

Tetranuclear Iron Carbonyl Complexes with a Central Tin Atom: Relationship to Iron Carbonyl Carbides

The energetics of CO dissociation from the lowest energy $E\text{Fe}_4(\text{CO})_n$ ($E = \text{C}, \text{Sn}; n = 16, 15, 14, 13$) structures account for the experimentally observed differences between the systems with central tin and central carbon atoms.

Xiaoli Gong, Liyao Zhu,* Jufeng Zhao,
Guangmang Cui, Xinmiao Lu,^a
Yaoming Xie, and R. Bruce King,*

